Coating Flows in a Nip Region and Various Critical Phenomena

When thin films of liquid are produced by roll coaters it is commonly observed that the liquid film is not uniform but shows either regular or irregular patterns resulting from hydrodynamic origins. The appearance of the liquid film has been considered to be governed by the flow geometry and dynamics in a nip region between two adjacent solid planes.

Experimental work was done to observe the flow geometries in the nip region and patterns of liquid film by using a roll-stationary, transparent flat plate system. Two fundamental mechanisms for rib disappearance in practical high-speed coatings were recognized. It was also found that the constant rib interval for infinite capillary number depends not only upon the minimum gap size but also upon the physical properties of the liquid. Experimental data are presented in dimensionless form for meniscus position, rib interval, constant rib interval, and for the critical or transient conditions of rib formation, rib disappearance, unstead ribbing, and centrifugal splash.

Comparison of present results for the speed ratio $U_2/U_1 = 0$ with previous results for $U_2/U_1 = 1$ shows the significance of the speed ratio to the meniscus position and the rib interval.

K. Adachi, T. Tamura, R. Nakamura
Department of Chemical Engineering
Kyoto University
Kyoto, 606, Japan

Introduction

The production of uniform films of liquid as a coating is a frequent industrial requirement; there are various methods for the purpose, but roll coating is by far the most widely used. When a thin film of liquid is transferred from a roll onto another roll or onto a web at an ordinary production speed, however, the coating film surface is not smooth but is covered by either a regular or an irregular pattern of hydrodynamic origin. If the place at which such a pattern occurs on the production line can be located, it may be possible to avoid or to overcome the trouble. However, it is often difficult to do so because of the lack of appropriate knowledge and data.

At the present stage of coating technology theoretical tools for analyses of coating phenomena are widely available, but there are few established results. The physical situation of interest here is the viscous flow past an air bubble in a narrow nip region between rolls, as shown in Figure 1. This type of flow is directly concerned with journal bearing lubrication as well as with roll coating. The basic flow is described well by the Reynolds lubrication equation; however, the boundary conditions at the bubble-fluid interface were a subject of discussion for many years, as reviewed by Taylor (1974) and Savage (1977a).

Two distinct lines of approach have been proposed, by Floberg (1965) and by Pearson (1960), to analyze the flow with a rib pattern of regularly spaced thick lines. Floberg regarded ribbed flow as a basic flow that can be described as three-dimensional lubrication flow. Pearson considered ribbed flow to be a perturbation of two-dimensional lubrication flow, and using a linear perturbation analysis on the basis of hydrodynamic stability theory, he explained the ribbing phenomenon for a wedge-plate configuration. His approach was revised by Pitts and Greiller (1961) and by Savage (1977b) using Coyne-Elrod conditions to predict the critical condition of rib instability and the rib interval for a two-roll configuration more precisely. Their theoretical predictions seem to be useful, but they do not cover a wide range of flow and operating conditions.

The flow rate through the nip, q, and the thickness of liquid film, h_∞, have been studied by Greener and Middleman (1975, 1979) for the case of two rolls rotating at equal speeds. The effects of different speeds on q and h_∞ have been investigated by Benkreira et al. (1981) experimentally, by Savage (1982) using a lubrication flow model, and by Coyle et al. (1986) by means of

Correspondence concerning this paper should be addressed to K. Adachi.

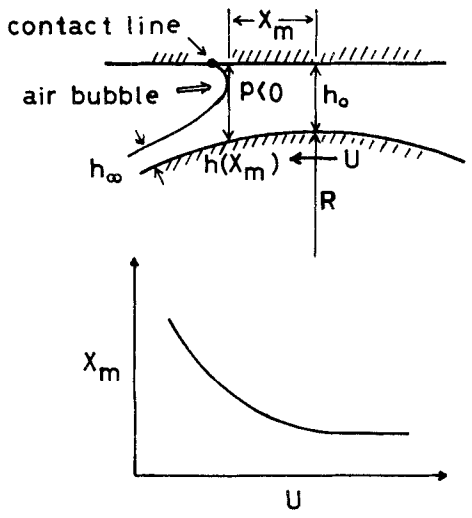

Figure 1. (a) Lubrication flow model. (b) Model prediction of meniscus position.

a finite-element simulation. Their results are almost consistent with each other.

The position of the meniscus, or the film-split location X_m, has been investigated by Pitts and Greiller (1961) and by Coyle et al. (1986) for a two-roll configuration. However, the effects of different diameters and speeds should be examined empirically as well. There also seem to be no reliable results about the position of the contact line and the contact angle for the relevant flow. In studying the boundary conditions at the film-split location, the ratio of film thickness to gap size at the meniscus position, $h_\infty/h(X_m)$, has been given by McEwan and Taylor (1966), Coyne and Elrod (1970), Saito and Scriven (1981), and Ruschak (1982). All the results are in good agreement for two equal size rolls rotating at equal speeds.

The critical conditions of rib onset at low capillary numbers have been studied for a two-roll configuration by Pitts and Greiller (1961), Mill and South (1967), Greener et al. (1980), Benkreira et al. (1982), Savage (1984), and Coyle et al. (1986). Their results are not convergent. Corresponding results for a roll-plate configuration have been presented by Savage (1977b) and Bauman et al. (1982). It is not clear if there is a definite difference between the two corresponding critical conditions. However, this ambiguity may not be a real problem for usual practical coatings because the roll speeds are much higher than the critical speeds.

The number of ribs per centimeter, which is the reciprocal of rib interval, has been studied experimentally by Mill and South (1967) for a system of two rolls with the same diameters and speeds, and theoretically as well as experimentally by Savage (1977b) for a roll-plate system. However, agreement between the theoretical and experimental results due to Savage has not been obtained in a range of intermediate and high capillary numbers. Moreover, the effect of the speed ratio U_2/U_1 on the rib interval λ has not yet been investigated, and it is also indeterminate what the constant rib interval λ_∞ for infinite capillary number depends upon, although Pulkrabek and Munter (1983) considered it to be a function only of the gap size h_0.

A short review of previous related work indicates that further reliable experimental data on coating flows are needed. Particularly, the effect of speed ratio on coating flow phenomena in high-speed coating should be investigated; moreover, one must understand how the film surface pattern is caused by the flow in a nip region. The appearance of the coating film surface is expected to depend decidedly on the positions of the meniscus and the contact line, which are formed in a nip region between rolls, because both are important parameters of flow geometry. These two quantities are difficult to observe directly for a practical two-roll system. Thus the purpose of the present work is to observe the positions of meniscus and contact line through the static, transparent plate of a roll-plate apparatus as Floberg (1965) did. In this system, the plate is stationary and so the speed ratio is zero. This value is far different from the value of 0(1) for practical coating. However, the data for this limiting case will be useful to show clearly the effect of speed ratio when compared with previous results for two-roll, equal-speed apparatus. It should be also remarked that the present system of $U_2/U_1 = 0$ is located at the middle point between the two-roll system in a forward rotation of $U_2/U_1 > 0$ and a system in a reverse rotation of $U_2/U_1 < 0$. As will be found later, the present results are related not only to forward coatings but also to reverse coatings.

The results of the present experimental work contain not only the data on the position of the meniscus and on the rib interval but also those on the critical conditions of rib onset, rib fluctuation, rib disappearance at high capillary numbers, and centrifugal splashing of coating liquid. Moreover, it has been observed that rib disappearance is caused by the combination of a displacement of contact line with a change in contact angle. The contact line and thus the meniscus could move even beyond the minimum gap point into the inlet nip region of converging flow. This phenomenon cannot be understood with an ordinary model of lubrication flow, but it seems to result from the dynamic wettability of the stationary plate with a coating liquid.

It will be useful for understanding the present experimental results to recall what ordinary lubrication theory predicts about the meniscus position and what Savage (1977a) presented as the critical condition for onset of the ribbing instability. Lubrication theory predicts a negative pressure in the diverging flow section. As the roll speed increases, the pressure lowers and it sucks the cylindrical air bubble more deeply into the nip region, as shown in Figure 1a. Thus the meniscus distance X_m and the gap size at the meniscus $h(X_m)$ decrease, and the curvature of the tip of the air bubble increases. When the gap size decreases sufficiently and so the curvature of the meniscus (or the corresponding negative pressure) exceeds a critical value that depends upon the flow conditions, the rib pattern suddenly appears on the coated plane. Then Savage's criteria for the onset of ribbing, which are similar to those of Pitts and Greiller (1961), determines the critical value. As X_m decreases, the effective length of the diverging flow section decreases, and consequently a further growth of the negative pressure will be suppressed. Then a deeper intrusion of the wedgelike, cylindrical air bubble ceases and X_m is expected to approach a positive limiting constant. Thus the ordinary model of lubrication flow predicts such a behavior, as shown in Figure 1b for the meniscus position. However this prediction will be found to be incomplete for highly viscous fluids from the present experimental fact mentioned before.

Experimental Method

A visual experiment was carried out to investigate the relation between the pattern of a coating film and its flow geometry in

the nip region. The apparatus consists of a roll and a flat plate, as illustrated in Figure 2. The top plate is of acryl and is transparent; the bottom roll is of chrome-plated steel and is 30 cm in both diameter and width. The plate was oriented horizontally and fixed rigidly to the side frames. The roll was set up horizontally and parallel to the plate so that the roll axis was just under the centerline of the plate ($x = 0$). The roll was mounted in bearing blocks that were moved vertically in the side frames by slide cotters with screws. The screws were used to adjust the gap size h_0 between the roll and the plate to selected values. The roll was driven by a variable-speed electric motor equipped with an automatic rotational speed controller. The rotational speed was measured by a digital counter connected to the shaft of the roll; it covered the range of 1 to 500 rpm, and the peripheral speed U was in the range of 0.0157 to 7.85 m/s. The gap between the roll and the plate was measured with a feeler gauge, and was varied between 0.03 and 1 mm.

Experiments were made with seven silicone oils covering a viscosity range from 0.00052 to 31.8 Pa · s. The physical properties of the liquids are given briefly in Table 1. The silicone oils designated 10P, 100P, and 300P showed shear thinning behaviors, so their viscosities were estimated at the characteristic shear rates of U/h_0 in correlating their experimental data. The other liquids were Newtonian, and their viscosities depended only upon liquid temperatures. The temperature was measured with a thermocouple inserted into the liquid in the inlet nip region.

When a small amount of coating liquid is poured over the running roll from a beaker, a part of it is used to form a thin liquid film coating the steel roll, another part is kept between the roll and the plate to form the menisci, and the rest rolls down from the inlet side of the nip, sparkling like mercury drops. Almost steady flows can be made easily without providing the coating liquid steadily, although occasional feeds are needed.

The meniscus and the contact line on the exit side of the nip are important because they have strong effects on various patterns on the coating film surface. Photographs of the nip flow were taken from above through the transparent top plate, and

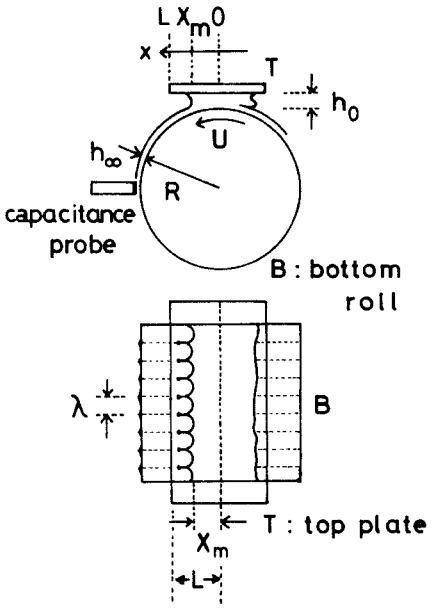

Figure 2. Experimental apparatus and dimensions.

Table 1. Physical Properties of Liquids

Silicone Oils	μ^* Pa · s	σ^* N/m	ρ^* kg/m^3
0.005P	0.00052	0.016	750
0.03P	0.0026	0.018	851
0.05P	0.0045	0.019	920
0.5P	0.052	0.020	962
1.5P	0.134	0.021	966
10P	1.07**	0.021	974
100P	9.3**	0.021	980
300P	31.8**	0.021	984

*Measured at 25°C
**Zero shear viscosity

the regular rib interval λ and the position of the meniscus line X_m were determined from the photographs. Displacement of the contact line and change in the contact angle were also observed, although the contact angle could not be measured even qualitatively. In order to obtain the film thickness of liquid on the roll, h_∞, a capacitance probe was used. The location of the probe is shown in Figure 2. Measured film thicknesses were in the range of 20 μm to 1 mm.

The experimental data are presented in the next section using the following variables in order to relate the present data to those for two-roll systems:

$$\bar{R} = 2R_1R_2/(R_1 + R_2) \tag{1}$$

$$\bar{U} = (U_1 + U_2)/2 \tag{2}$$

$$U_2/U_1$$

where $\bar{R}$ is the mean roll radius, $\bar{U}$ the averaged speed, and U_2/U_1 the speed ratio. The roll-stationary plate system under investigation is a special case of two different size rollers rotating at different speeds. The top plate can be regarded as a stationary roll of infinite radius: $R_2 = \infty$ and $U_2 = 0$. Thus, the present case is expressed by

$$\bar{R} = 2R,\ \bar{U} = U/2,\ U_2/U_1 = 0 \tag{3}$$

The most important dimensionless parameter for the data presentation is the capillary number, defined by

$$Ca = \mu\bar{U}/\sigma \tag{4}$$

The reason is that the viscous drag $\mu U/h_0$ and the surface tension σ/h_0 are dominant for a thin liquid film although, in general, the following three forces also possibly act upon the fluid motion: the force of inertia ρU^2, the gravity $\rho g h_0$, and the centrifugal force $\rho U^2 h_0/R$.

Results and Discussion

Most of the present experimental data were obtained during the ribbing state. However it was observed that the film thickness h_∞ and the meniscus position X_m did not change strikingly between before and after the onset (or the disappearance) of ribbing. Ribbing was much affected by X_m but the latter was hardly influenced by the former. Another point to be mentioned is that the phenomenon of rib disappearance at high capillary

numbers was not always observed for a coating liquid of low viscosity because of an earlier occurrence of centrifugal splash.

Film thickness and meniscus position

The experimental data of the flow rate, q, were made dimensionless with $h_0\bar{U}$ and plotted in Figure 3 against the capillary number defined by Eq. 4. It must be noted here that this nondimensional flow rate α can be related to the dimensionless film thickness h_∞/h_0 as explained in the Appendix. For a roll-stationary plate system,

$$\alpha \equiv q/h_0\bar{U} = 2(h_\infty/h_0) \tag{5}$$

The data points show no dependence upon capillary number. The averaged value is around 1.2, although the values are somewhat scattered owing to an inappropriate system of measurement and calibration with the capacitance probe. The value of $\alpha = 1.2$ is in general agreement with those of previous investigators. The experimental results of Sullivan and Middleman (1979) ranged from $\alpha = 1.1$ to 1.3, and the theoretical estimation of Coyle (1984) on the basis of a finite-element simulation gave $\alpha = 1.23$ for an infinite capillary number. The data and analysis of Greener and Middleman (1979) also show $\alpha = 1.3$ for a system of two equal-size rollers rotating at equal speeds. Even for two different size rollers rotating at different speeds, the experiments of Benkreira et al. (1981) showed that $\alpha = 1.31$ in forward rotation and $\alpha = 1.26$ in reverse rotation. Thus it has been found that the dimensionless flow rate α is very insensitive to a change in the flow situation.

The meniscus position X_m is a primary factor influencing the phenomena of coating flow since it determines the flow geometry in the nip region. A general correlation of the present experimental data between the dimensionless meniscus position, $X_m/(h_0\bar{R})^{1/2}$, and capillary number has been made and is shown in Figure 4 for the case of $U_2/U_1 = 0$. The data points show not a little amount of scatter, but they can be roughly represented by a single solid line. This line is in general agreement with the broken line, the empirical result of Floberg (1965), although not a little discrepancy is seen at low capillary numbers. As roll speed increases, the meniscus position or distance X_m decreases sharply at low capillary numbers and gradually at intermediate capillary numbers, as anticipated from the lubrication flow model described in the Introduction. However, contrary to this anticipation the data do not show the existence of a positive lower limit. As roll speed increases further, X_m decreases again rapidly at high capillary numbers, and the tip of the meniscus enters beyond the minimum gap point ($X = 0$) even into the converging flow region on the inlet side of the nip. This phenomenon

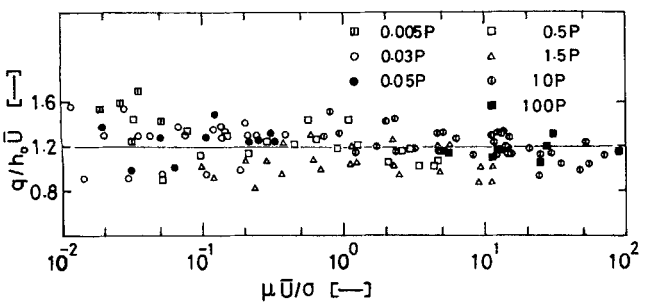

Figure 3. Dimensionless flow rate vs. capillary number.

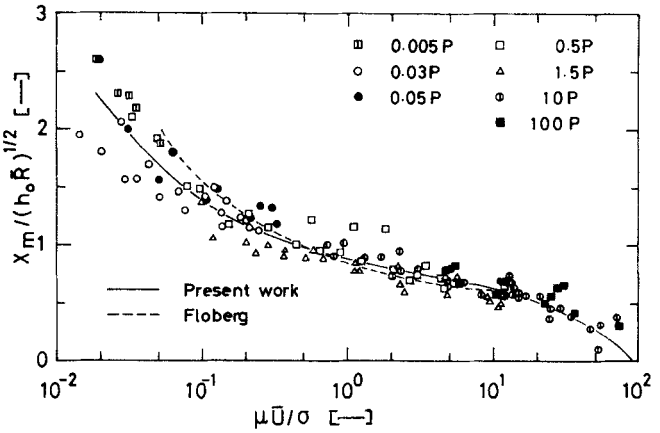

Figure 4. General relation between dimensionless meniscus position and capillary number.
Case of $U_2/U_1 = 0$

is not explained as the action of the negative pressure due to lubrication flow because no negative pressure exists in the converging flow region, and so a rational explanation will be given later in relation to rib disappearance at high capillary numbers. It should be also mentioned that the experimental data of X_m will be found useful even in other practical coatings than roll coatings, as described in the next section.

The present empirical result on X_m is compared in Figure 5 with the theoretical result of Coyne and Elrod (1970) for $U_1/U_2 = 0$. The agreement between both is satisfactory, and the small discrepancy at high capillary numbers is also reasonable because Coyne and Elrod did not take into account displacement of a contact line (point A in Figure 14, Appendix). Figure 5 also shows a comparison in X_m between the two cases of $U_2/U_1 = 0$ and 1. It must be mentioned here that the theoretical predictions of Coyne and Elrod (1970) could be applied to the two relevant cases, as seen in Figure 5 and as will be explained in detail in the Appendix, although they treated only a special case of roll-plate configurations. The predictions of Coyne and Elrod and of Ruschak (1982) have been obtained from their theoretical results of $H(X_m)/H_\infty$ using the following relation with $\alpha = 4/3$:

$$X_m/(h_0\bar{R})^{1/2} = [\alpha H(X_m)/H_\infty - 1]^{1/2} \tag{6}$$

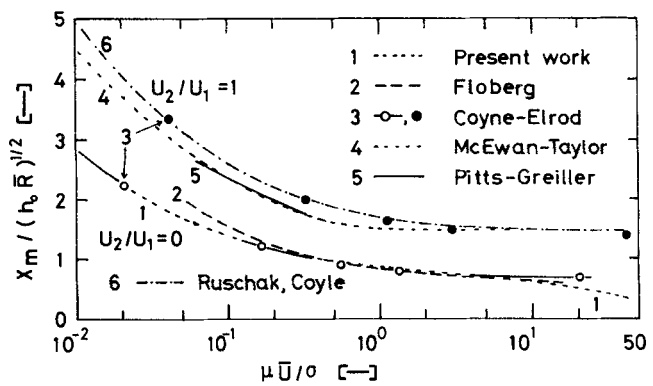

Figure 5. Difference in dimensionless meniscus position.
Cases of $U_2/U_1 = 0$ and 1

McEwan and Taylor (1966) also determined $H(X_m)/H_\infty$ performing an experimental study on peeling an adhesive tape, and this quantity has been transformed into dimensionless meniscus position in the same way. Pitts and Greiller (1961) gave the experimental data of $H(X_m)/H_0 (\equiv h(X_m)/h_0)$ in the case of two rolls of equal size rotating at equal speeds, and this quantity has been transformed into the relevant quantity using the following gap size function;

$$h(X)/h_0 = 1 + [X/(h_0\bar{R})^{1/2}]^2 \tag{7}$$

The comparison between the two cases of $U_2/U_1 = 0$ and 1 demonstrates that the effect of the speed ratio U_2/U_1 on the dimensionless meniscus position is rather significant, so that it should be investigated further over a wider range of speed ratio. Another point to be remarked is that the dimensionless meniscus position for $U_2/U_1 = 1$ attains a lower limit at high capillary numbers, although that for $U_2/U_1 = 0$ decreases gradually with increasing capillary number. This difference results from the difference that a contact line does not exist in the former case but on the contrary it does exist in the latter case, as is the case in reverse roll coating. The contact line moves toward the inlet diverging flow region with increasing capillary number as described later, so that the meniscus also moves more or less in the same direction.

Steady ribbing, rib onset, and rib disappearance

Rib intervals λ were quite long just after the onset of ribbing, but they decreased rapidly with increasing roll speed and then they approached constant values λ_∞, as reported by Mill and South (1967) for two-roll systems. It was found from present experimental data that the following relation holds approximately

$$\lambda_\infty/h_0 \propto (h_0/\bar{R})^{-1/3} \tag{8}$$

Using this relation, all the experimental data of λ_∞ for the same fluid can be reduced to those of a constant value irrespective of $h_0/\bar{R}$. Thus a general relation between the dimensionless rib interval $\lambda/(h_0^2\bar{R})^{1/3}$ and capillary number has been made for the case of $U_2/U_1 = 0$, as shown in Figure 6. Any empirical curve of λ, which is similar to the curve in Figure 1b, falls down sharply, touches with the solid straight line, and then connects with a branch of the horizontal lines, as the capillary number increases. The constant value of $\lambda_\infty/(h_0^2\bar{R})^{1/3}$ on each horizontal line depends mainly upon the physical properties of liquid, so each branch has been distinguished by the following subsidiary dimensionless parameter

$$Ro \equiv \mu^2 g\bar{R}/\sigma^2 \tag{9}$$

This parameter was selected for a monotonous relation between $\lambda_\infty/(h_0^2\bar{R})^{1/3}$ and Ro, as shown later, although we have not yet found its physical basis.

The present empirical curve, the solid line in Figure 6, is in perfect agreement with the empirical result of Floberg (1965), in a wide range of $Ca > 0.5$, shown by the broken line. The present experimental data are also consistent with those of Savage (1977b) in general. The data points at low capillary numbers, where the slope of the empirical curve of λ is steep, include apparent dependence of dimensionless rib interval on the gap size h_0, so those data points appear to be more scattered than experimental errors. However the scattering of the data points at low capillary numbers is not always a serious defect of the present correlation because industrial coating operations are usually made in a region that rib intervals are almost independent of roll speeds. The solid straight line and horizontal lines are useful in the present correlation chart, because the dependence of λ and X_m on h_0 is not revealed in usual coatings owing to both narrow ranges of small gap sizes and high production speeds.

A correlation chart between the dimensionless constant rib interval $\lambda_\infty/(h_0^2\bar{R})^{1/3}$ and the dimensionless parameter $\mu^2 g\bar{R}/\sigma^2$ has been made and is shown in Figure 7. The present results (solid line) are compared with those of Floberg (1965) (broken line) for $U_2/U_1 = 0$. There is a large discrepancy for less viscous liquids. One reason for this may be that the data of Floberg in the relevant correlation have not always attained sufficiently limiting constants λ_∞. The results for $U_2/U_1 = 0$ are compared in the same figure with the results of Mill and South (1967) for $U_2/U_1 = 1$. They have stated that the rib interval for two rolls rotating at equal speeds is independent of fluid properties as well as speeds at higher capillary numbers than 1.2, and considered that this constant rib interval λ_∞ depends solely upon h_0 and $\bar{R}$. Pulkrabek and Munter (1983) regarded λ_∞ as a function only of h_0, and they gave it as a straight line in their data correlation chart. This line is expressed by

$$\lambda_\infty \propto h_0^{0.79} \tag{10}$$

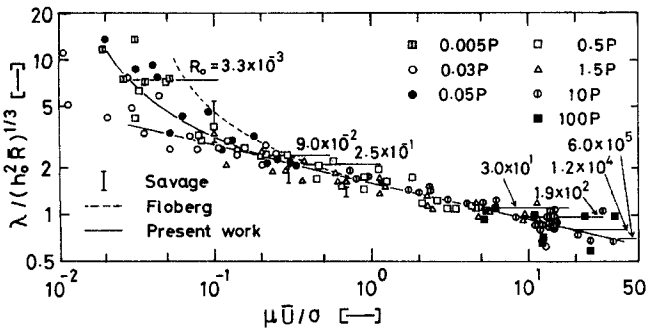

Figure 6. General relation between dimensionless rib interval and capillary number.
Case of $U_2/U_1 = 0$

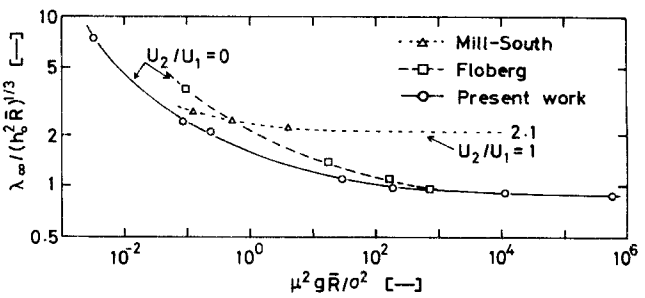

Figure 7. Dependence of constant rib interval at high capillary numbers upon fluid properties and mean roll radius.

and it is only a little different from the present result

$$\lambda_\infty \propto h_0^{2/3} \tag{11}$$

However Figure 7 shows clearly the dependence of λ_∞ on fluid properties. The large difference in dimensionless constant rib interval between the two relevant cases is considered to result mainly from the corresponding difference in meniscus position in Figure 5.

A comment related to rib interval should be made regarding the experimental work of Fukada et al. (1961) since it has often been referred to. They observed a regular stripe pattern similar to the rib pattern but abnormally wide in the stripe interval. They reported that the regular stripe interval does not vary with changing roll speed for Newtonian liquids and that this constant stripe interval increases with increasing viscosity as well as gap size. The increase in the constant stripe interval with increasing viscosity is entirely opposite to one of the present findings, and their stripe interval is extraordinarily wide when compared with the usual interval for a highly viscous liquid. Thus the stripe pattern observed by Fukada et al. must be considered to result from a cause more or less different from that of the ordinary ribbing phenomenon.

As illustrated in Figures 2 and 9a, the tip of the wedgelike cylindrical air bubble in the exit nip region is divided by liquid films with regular spacing at the instant when the roll speed exceeds a critical value, as described in the Introduction. This transition point was determined by observing the meniscus shape. The meniscus line observed from above was a straight line at the beginning; it became a wavy line and then toothed or comblike with increasing speed. It should be noted that this direct detection of ribbing instability is superior to indirect detection of a rib pattern on the roll, since the rib pattern is obscure owing to the leveling phenomenon striking at the low roll speed as well as owing to the very wide rib interval at a transition point.

The present experimental results on the critical condition for ribbing instability are shown in Figure 8 and are compared with various existing results for both $U_2/U_1 = 0$ and $U_2/U_1 = 1$. The present data points, denoted by solid circles, are only a little above the experimental and the theoretical curves, 2 and 3, respectively, given by Savage (1977b) for $U_2/U_1 = 0$, and the present empirical line is found to be consistent with the empirical curve, no. 1, presented by Bauman et al. (1982) if one takes into account that the slopes of almost all the curves become milder as $h_0/\bar{R}$ decreases. The other curves in Figure 8, nos. 4 to 11, are the results for $U_2/U_1 = 1$. The two empirical results of Mill and South (1967) and Pitts and Greiller (1961), represented respectively by lines 7 and 8, are in good agreement with the theoretical prediction of Savage (1984) given by line 10. However, empirical curve no. 6 presented by Benkreira et al. (1982) and the empirical and theoretical curves, nos. 5 and 9, given by Coyle (1984) are much above the rest in a range of small gap size. The above experimental results for $U_2/U_1 = 1$ may indicate that the observed critical speed decreases with decreasing roll diameters, since the mean diameters of the two rolls were 200–100 mm for Benkreira et al., 200–76.2 mm for Coyle, 65.8–49.5 mm for Mill and South, and 50.8–25.4 mm for Pitts and Grellier. Then results obtained with rolls of smaller diameters seem to be more reliable in a range of $h_0/\bar{R}$ of low values, taking account of the difficulty in the detection of the

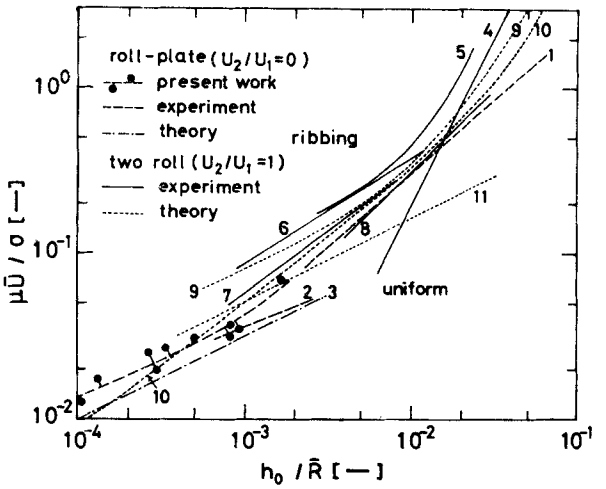

Figure 8. Critical capillary number for onset of ribbing at low capillary numbers.

1. Bauman et al. (1982)
2,3. Savage (1977b)
4. Greener et al. (1980)
5,9. Coyle (1984)
6, 11. Benkreira et al. (1982)
7. Mill and South (1967)
8. Pitts and Greiller (1961)
10. Savage (1982)

onset of ribbing for two-roll systems as mentioned before. Thus it can be guessed roughly that the difference in the critical capillary number between the two cases of $U_2/U_1 = 0$ and 1 will not be significant.

Rib disappearance is another expression of the same phenomenon as the onset of ribbing, and it was observed at both high and low capillary numbers. When roll speed was decreasing at low capillary numbers, the rib pattern suddenly became invisible, owing to a widening of rib interval. As roll speed increased at high capillary numbers, the rib pattern gradually disappeared owing to a decrease in rib height at a constant rib interval. It was observed that the decrease in rib height was caused by an increase in the contact angle, θ_c, and by a displacement of the contact line toward the inlet nip region, as illustrated in Figure 9. Coyle et al. (1966) have shown that such a displacement of contact line results from the increase in contact angle. Similar phenomena are often seen also in reverse roll coatings. Thus it can be concluded that the rib disappearance at a high capillary number is caused by the decrease in dynamic wettability. Attention should be paid here to the fact that the critical condition for

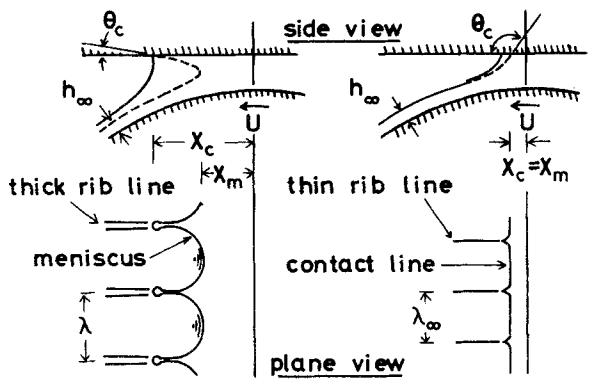

Figure 9. Observations of contact angles and ribs.

(a) Thick and high ribs
(b) Thin and low ribs, just before rib disappearance

the relevant rib disappearance will not be defined by the capillary number of a liquid alone. This phenomenon occurs at the solid-liquid interface, so that it must depend not only upon the surface tension of the liquid but also upon the physical properties of the solid surface concerned with the dynamic wettability.

It was difficult to measure the contact angle θ_c, and so only the position of the contact line can be determined from Figure 10 since the positions of the contact line and the meniscus were almost the same in the state of rib disappearance at high capillary numbers. The same figure also indicates that rib patterns disappear for viscous fluids under the condition that the dimensionless distance between the meniscus position and the minimum gap point is shorter than about 0.2. Figure 10 is inconvenient for predicting the critical speed of rib disappearance for a given operation condition. Another correlation chart is given in Figure 11, in which the solid line represents the critical condition for rib disappearance at high capillary numbers. Thin uniform films can be obtained at higher speeds than the critical ones at constant minimum gap sizes. It should be noted that $\bar{U}$ in the capillary number has been replaced by the relative velocity, ΔU, in the two correlation charts presented above because the dynamic wettability at the solid-liquid interface is considered to be governed not by the average velocity but by the velocity difference between the solid and the bulk liquid. Justification for this consideration seems to be given by observation of the air entrainment by a moving solid surface and by the fact that the relevant rib disappearance can be seen for the case of two rolls not in forward rotation at equal speed but only in reverse rotation with a large relative velocity difference.

As mentioned before, rib disappearance was observed at high and low capillary numbers, but was not observed at middle capillary numbers. However rib patterns always disappeared when the top plate was located at a position of $L \leq X_m$, where L is the distance from $X = 0$ to the exit end of the plate, as seen in Figure 2, and X_m is the empirical meniscus distance given in Figure 4. This phenomenon is understood to indicate that such a decrease in the length of the exit diverging flow section gives a negative pressure smaller than the critical pressure for the onset of ribbing corresponding to a given flow condition. This information

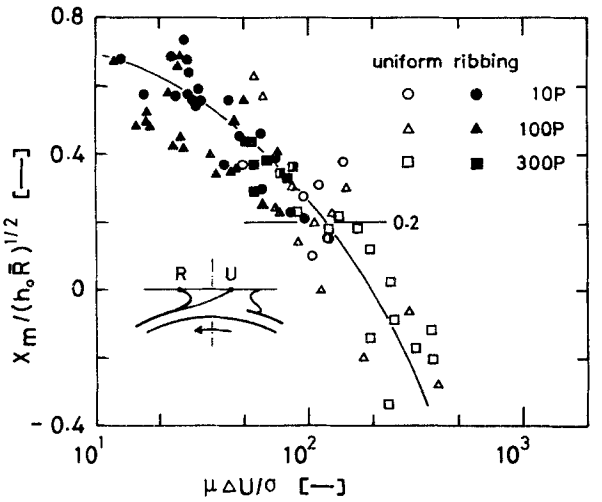

Figure 10. Critical meniscus position for rib disappearance at high capillary numbers.

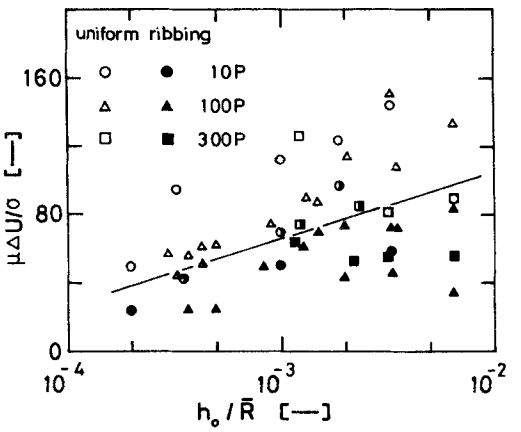

Figure 11. Critical operating conditions for rib disappearance at high capillary numbers.

and data will be useful for several types of coatings, such as blade, bar, and slot coatings.

Unsteady ribbing and centrifugal splash

In a range of higher capillary numbers than those for steady ribbing, either unsteady ribbing or centrifugal splash of a coating liquid was observed, or both were observed one after another. For unsteady ribbing, the meniscus fluctuated irregularly along the roll axis, so that the ribbing resulted in irregular, wavy stripe patterns. Figure 12 shows the experimental data on the critical condition for the onset of unsteady ribbing. Since Re = 10–90 for the present data, it has been assumed that unsteady ribbing occurs at the instant when the inertial force, $\rho\bar{U}^2$, becomes more significant than the viscous force, $\mu\bar{U}/h_0$, and the surface tension, σ/h, both of which are indispensable for steady ribbing flow. The experimental data on the critical condition for the onset of centrifugal splash are presented in Figure 13, where the dimensionless variable on the ordinate is the square root of the stress ratio of centrifugal force to surface tension. It has been assumed according to observations of splashing that the coating liquids of two rings at the edges of the cylindrical roll plane, which are thicker than the inside liquid film, splash when the centrifugal acceleration force, $\rho U^2 h_0/R$, exceeds a limit for the

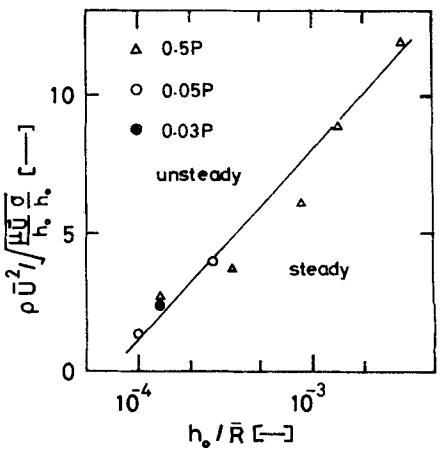

Figure 12. Critical conditions for onset of unsteady ribbing.

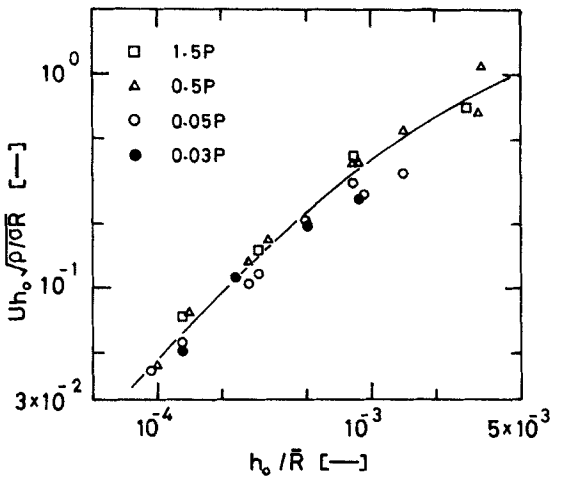

Figure 13. Critical conditions for onset of centrifugal splashing.

ring drop whose size almost depends upon the surface tension, σ/h_0. This is similar to the critical phenomenon for gravitational fall of a drop suspending from a horizontal plate. Coating liquid is predicted to splash when the value of the relevant dimensionless parameter exceeds a critical value specified for any given gap size by the solid line in Figure 13.

Conclusions

Present observations of the nip flow and the appearance of the film surface over the roll give the following results.

1. The speed ratio is expected to have a significant effect upon the regular rib interval as well as upon the position of the meniscus.

2. The constant rib interval for infinite capillary number depends not only upon the minimum gap size but also upon physical properties of the liquid, although the latter dependence is not striking for the case where *Ro* is greater than about 100.

3. At low capillary numbers the rib pattern becomes discernible because of a sudden shortening of rib interval, and this critical phenomenon seems to be caused by the dynamic instability due to surface tension. On the other hand, at high capillary numbers the rib pattern becomes indiscernible in such a way that the rib height decreases gradually at a constant rib interval with increasing capillary number. This transient phenomenon is considered to result from the decrease in the dynamic wettability at the liquid-top plate interface.

4. In practical high-speed coatings, there are two possible ways to let the rib pattern disappear. One way is to make the exit diverging flow region shorter than that of X_m given in Figure 4, as seen in blade coatings. The other way is to control the dynamic contact angle either by a mechanical method, as is the case in reverse roll coatings, or by a temporary modification of surface tension so that the curvature of the meniscus may be kept too low to cause the ribbing instability.

Notation

Ca = capillary number, $\mu\bar{U}/\sigma$
g = gravitational acceleration
H = half-gap size, Figure 15a
H_∞ = film thickness, Figure 15a
h = gap size, Figure 1a or Eq. 7
h_∞ = film thickness, Figure 1a
L = distance from $X = 0$ to exit end of plate
p = static pressure
q = volumetric flow rate per unit width of a roll
R = radius of a roll
Re = Reynolds number, $h_0\bar{U}\rho/\mu$
Ro = dimensionless parameter for constant rib intervals, $\mu^2 g\bar{R}/\sigma^2$
U = peripheral speed of a roll
ΔU = relative speed ($=|U_1 - U_2|$)
X = longitudinal coordinate
X_m = coordinate of meniscus position

Greek letters

α = dimensionless volumetric flow rate per unit width of a roll
λ = regular rib interval
λ_∞ = constant rib interval for infinite capillary number
μ = liquid viscosity
ρ = liquid density
σ = liquid surface tension

Subscripts

0 = value at point of minimum gap size
1,2 = quantity for each roll in a general two-roll system

Superscripts

$\bar{}$ = mean value, Eq. 1 or 2

Appendix

Coyne and Elrod (1970) analyzed the lubrication flow shown in Figure 14 and presented a numerical table of $H_\infty/H(X_m)$. The results can be applied to the two cases as follows.

A. Two equal-size rolls rotating at equal speeds

The flow field, which is surrounded by the boundary *ABCDE* in Figure 14, is regarded as similar to that in Figure 15a. The flow conditions for this case are

$$R_1 = R_2 = \bar{R} = R, \quad U_1 = U_2 = \bar{U} = U, \quad U_2/U_1 = 1$$
$$h_0 = 2H_0, \quad h_\infty = H_\infty, \quad h(X_m) = 2H(X_m), \quad q = 2H_\infty U \quad \text{(A1)}$$

where q is the volumetric flow rate per unit roll width through the nip. Then one can derive

$$Ca = \mu U/\sigma \quad \text{(A2)}$$

$$X_m/\sqrt{h_0\bar{R}} = \left[\alpha\frac{H(X_m)}{H_\infty} - 1\right]^{0.5} \quad \text{(A3)}$$

from Eq. 4 and

$$\alpha \equiv q/h_0\bar{U} = H_\infty/H_0 \quad \text{(A4)}$$

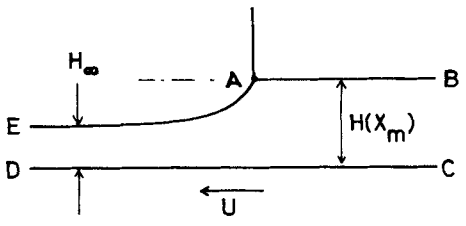

Figure 14. Lubrication flow model of Coyne and Elrod.

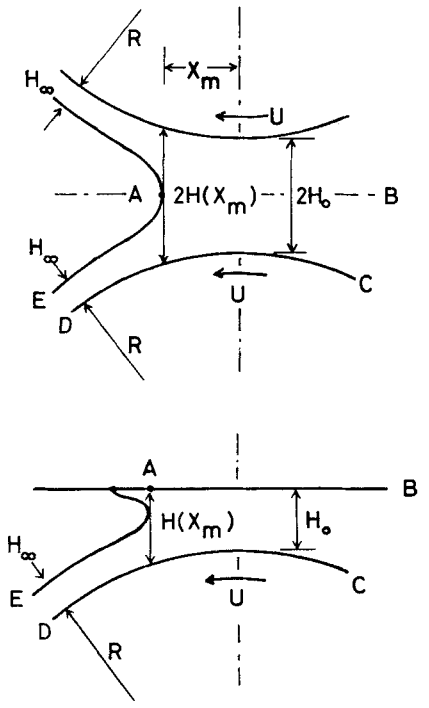

Figure 15. Application of Coyne and Elrod model.
(a) $U_2/U_1 = 1$
(b) $U_2/U_1 = 0$

$$1 + (X_m/\sqrt{h_0\bar{R}})^2 \simeq h(X_m)/h_0 = H(X_m)/H_0 \quad \text{for } |X_m/\bar{R}| \ll 1 \qquad \text{(A5)}$$

B. A roll and a stationary flat plate

The flow field, which is surrounded by the boundary *ABCDE* in Figure 14, is regarded as similar to that in Figure 15b. The flow conditions for this case are

$$R_1 = R, \quad R_2 = \infty, \quad \bar{R} = 2R$$
$$U_1 = U, \quad U_2 = 0, \quad \bar{U} = U/2, \quad U_2/U_1 = 0$$
$$h_0 = H_0, \quad h_\infty = H_\infty, \quad h(X_m) = H(X_m), \quad q = H_\infty U \qquad \text{(A6)}$$

Then the following relations

$$Ca = \mu U/2\sigma \qquad \text{(A7)}$$

$$X_m/\sqrt{h_0\bar{R}} = \left[\frac{\alpha}{2}\frac{H(X_m)}{H_\infty} - 1\right]^{0.5} \qquad \text{(A8)}$$

are deduced from Eq. 4 and

$$\alpha \equiv q/h_0\bar{U} = 2(H_\infty/H_0) \qquad \text{(A9)}$$

$$1 + (X_m/\sqrt{h_0\bar{R}})^2 \simeq h(X_m)/h_0 = H(X_m)/H_0 \quad \text{for } |X_m/\bar{R}| \ll 1 \qquad \text{(A10)}$$

It is well known that the dimensionless flow rate α is approximately $\frac{4}{3}$. Therefore this value was used together with the results of Coyne and Elrod (1970) in calculating the dimensionless meniscus position $X_m/(h_0\bar{R})^{0.5}$ by Eqs. A3 and A8. The final results are presented as those of Coyne and Elrod in Figure 5.

Literature Cited

Bauman, T., T. Sullivan, and S. Middleman, "Ribbing Instability in Coating Flows: Effect of Polymer Additives," *Chem. Eng. Commun.*, **14,** 35 (1982).

Benkreira, H., M. F. Edwards, and W. L. Wilkinson, "Roll Coating of Purely Viscous Liquids," *Chem. Eng. Sci.*, **36,** 429 (1981).

———, "Ribbing Instability in the Roll Coating of Newtonian Fluids," *Plast. Rubber Proc. Appl.*, **2,** 137 (1982).

Coyle, D. J., "The Fluid Dynamics of Roll-Coating: Steady Flows, Stability and Rheology," Ph.D. Thesis, Univ. Minnesota (1984).

Coyle, D. J., C. W. Macosko, and L. E. Scriven, "Film Splitting Flows in Forward Roll Coating," *J. Fluid Mech.*, **171,** 183 (1986).

Coyne, J. C., and H. G. Elrod, "Conditions for the Rupture of a Lubricating Film. I: Theoretical Model," *J. Lubr. Tech.*, **73,** 451 (1970).

Floberg, L., "On Hydrodynamic Lubrication with Special Reference to Sub-Cavity Pressures and Number of Streamers in Cavitation Regions," *Acta Polytech. Scad.*, **ME19,** (1965).

Fukada, E., M. Fukushima, and T. Sone, "An Anomalous Flow During Rolling of Viscous Materials," *Rept. of Kobayashi Rigaku Kenkyusho (Japan)*, **11**(1,2), 36 (1961).

Greener, J., and S. Middleman, "A Theory of Roll Coating of Viscous and Viscoelastic Fluids," *Polym. Eng. Sci.*, **15,** 1 (1975).

———, "Theoretical and Experimental Studies of the Fluid Dynamics of a Two-Roll Coater," *Ind. Eng. Chem. Fundam.*, **18,** 35 (1979).

Greener, J., T. Sullivan, B. Turner, and S. Middleman, "Ribbing Instability of a Two-Roll Coater: Newtonian Fluids," *Chem. Eng. Commun.*, **5,** 73 (1980).

McEwan, A. D., and G. I. Taylor, "The Peeling of a Flexible Strip Attached by a Viscous Adhessive," *J. Fluid Mech.*, **26,** 1 (1966).

Mill, C. C., and G. R. South, "Formation of Ribs on Rotating Rollers," *J. Fluid Mech.*, **28,** 523 (1967).

Pearson, J. R. A., "The Instability of Uniform Viscous Flow Under Rollers and Spreaders," *J. Fluid Mech.*, **7,** 481 (1960).

Pitts, E., and J. Greiller, "The Flow of Thin Liquid Films between Rollers," *J. Fluid Mech.*, **11,** 33 (1961).

Pulkrabek, W. W., and J. D. Munter, "Knurl Roll Design for Stable Rotogravure Coating," *Chem. Eng. Sci.*, **38,** 1309 (1983).

Ruschak, K. J., "Boundary Conditions at a Liquid/Air Interface in Lubrication Flows," *J. Fluid Mech.*, **119,** 107 (1982).

Saito, H., and L. E. Scriven, "Study of Coating Flow by the Finite-Element Method," *J. Comput. Phys.*, **42,** 53 (1981).

Savage, M. D., "Cavitation in Lubrication. 1: On Boundary Conditions and Cavity-Fluid Interfaces," *J. Fluid Mech.*, **80,** 743 (1977a).

———, "Cavitation in Lubrication. 2: Analysis of Wavy Interfaces," *J. Fluid Mech.*, **80,** 757 (1977b).

———, "Mathematical Models for Coating Processes," *J. Fluid Mech.*, **117,** 443 (1982).

———, "Mathematical Model for the Onset of Ribbing," *AIChE J.*, **30,** 999 (1984).

Sullivan, T. M., and S. Middleman, "Roll Coating in the Presence of a Fixed Constraining Boundary," *Chem. Eng. Commun.*, **3,** 469 (1979).

Taylor, C. M., "Film Rupture for a Lubricated Cylinder Lightly Loaded against a Plane," *J. Mech. Eng. Sci.*, **16,** 225 (1974).

Manuscript received Apr. 24, and revision received Sept. 8, 1987.